JASS Journal of Astronomy and Space Sciences

Laser-based Relative Navigation Using GPS Measurements for Spacecraft Formation Flying

Kwangwon Lee[1], Hyungjik Oh[1], Han-Earl Park[2], Sang-Young Park[1†], Chandeok Park[1]

[1]Astrodynamics & Control Laboratory, Department of Astronomy, Yonsei University, Seoul 03722, Korea
[2]Korea Astronomy and Space Science Institute, Daejeon 34055, Korea

This study presents a precise relative navigation algorithm using both laser and Global Positioning System (GPS) measurements in real time. The measurement model of the navigation algorithm between two spacecraft is comprised of relative distances measured by laser instruments and single differences of GPS pseudo-range measurements in spherical coordinates. Based on the measurement model, the Extended Kalman Filter (EKF) is applied to smooth the pseudo-range measurements and to obtain the relative navigation solution. While the navigation algorithm using only laser measurements might become inaccurate because of the limited accuracy of spacecraft attitude estimation when the distance between spacecraft is rather large, the proposed approach is able to provide an accurate solution even in such cases by employing the smoothed GPS pseudo-range measurements. Numerical simulations demonstrate that the errors of the proposed algorithm are reduced by more than about 12% compared to those of an algorithm using only laser measurements, as the accuracy of angular measurements is greater than 0.001° at relative distances greater than 30 km.

Keywords: formation flying, global positioning system (GPS) measurement, laser measurement, relative navigation, extended Kalman filter (EKF)

1. INTRODUCTION

The relative navigation algorithm plays a key role in implementing spacecraft formation flying, since the accuracy of the navigation solution is critically related to mission specification. The accurate navigation solutions allow us to operate challenging missions such as precise measurements of Earth's gravity field, detection of gravitational waves, and 3-dimensional mapping. Thus, various approaches to relative navigation have been developed for about a decade, and are generally based on the Global Positioning System (GPS) measurements. Montenbruck et al. (2002) suggested a kinematic navigation algorithm for relative positioning using single differences of smoothed pseudo-range measurements. Kroes et al. (2005) developed a real-time navigation algorithm to estimate relative states via the Extended Kalman Filter

(EKF) using single differences of pseudo-range and carrier-phase measurements with the Least squares AMBiguity Decorrelation Adjustment (LAMBDA), and it was validated in the Gravity Recovery And Climate Experiment (GRACE) mission. Leung and Montenbruck (2005) designed a navigation system to estimate absolute and relative states of multiple formation flying satellites via multiple Kalman filters. Ardaens et al. (2010) presented flight results of relative GPS-based navigation for the PRISMA mission. Park et al. (2010) and Park et al. (2013) validated a GPS-based navigation algorithm through a Hardware-In-the-Loop (HIL) testbed including GPS signal generators and receivers.

Recently, laser instruments have attracted much attention for space missions with scientific goals, since they are geared toward precisely measuring distances between two objects. Several conceptual system designs using laser instruments in space missions have been proposed, such

as the Laser Interferometer Space Antenna (LISA) and GRACE follow-on mission (Shaddock 2008; Sheard et al. 2012). This attention has also led to the development of a precise navigation algorithm based on laser measurements only. Wang et al. (2011) proposed an adaptive Huber filter algorithm for a laser radar navigation system in formation flying. Jung et al. (2012) formulated a relative navigation algorithm via EKF based on laser ranging. These approaches are capable of precisely estimating relative states when spacecraft are closed to one another, but they require obtaining azimuth/elevation angles representing the orientation of the relative position vector (i.e., the direction in which the laser is pointing). Since the angular information inherently depends on the accuracy of spacecraft attitude estimation, these approaches might yield an inaccurate solution in large-scale formation flying, which involves baselines of tens to hundreds of kilometers, even with reasonable attitude estimation. In the case of attitude estimation, even though a spacecraft has high-accuracy sensors for attitude determination, small spacecraft might be unable to load highly accurate sensors covering all Field of View (FOV) because of its dimensional constraints. That is, the issue of inaccurate attitude estimation is practically possible. Moreover, azimuth and elevation errors must be greater than or equal to the attitude estimation errors, since numerical and systematic errors might be accumulated through the coordinate transformations.

This study presents a combined navigation algorithm for large-scale formation flying by employing both laser and GPS pseudo-range measurements. Based on the algorithmic structure proposed in Jung et al. (2012), the single difference of pseudo-range measurements between two receivers smoothed by carrier phase measurements are incorporated into the measurement model, instead of azimuth and elevation angles, to overcome the limited accuracy due to the attitude estimation errors. While the navigation algorithm using only laser measurements depends on the accuracy of attitude estimation, this proposed approach based on the combined laser/GPS measurement model is independent of attitude estimation by excluding angular measurements of laser direction. Thus, its accuracy can be superior to those navigation algorithms that only use laser measurements, especially in the case of large-scale spacecraft formation flying with poor (or even reasonable) attitude estimation.

The overall discussion begins with the modification of the measurement model by employing GPS pseudo-range measurements after introducing the relative navigation algorithm via EKF in spherical coordinates based on Jung et al. (2012). Simulation results in large-scale formation flying are then presented to demonstrate the advantage of the proposed approach. Analyses of the relative navigation strategy using laser measurements are followed by the conclusion.

2. METHODOLOGY

2.1 Relative Navigation Algorithm in Spherical Coordinates

The relative navigation algorithm using laser measurements with respect to a chief satellite is usually defined in spherical coordinates, since they well represent the nature of laser ranging in relative motion. The spherical coordinates stated in Jung et al. (2012) are defined by ρ, θ, and ϕ, and are shown in Fig. 1. The variable ρ is the relative distance between the chief and deputy, and θ and ϕ are the azimuth and elevation angles, respectively. The coordinate transformation between rectangular and spherical coordinate in relative motion can be stated as follows (Jung et al. 2012):

$$x = \rho \cos\theta \cos\phi$$
$$y = \rho \sin\theta \cos\phi$$
$$z = \rho \sin\phi \qquad (1)$$

Similar to Jung et al. (2012), the relative navigation algorithm via EKF (Kalman 1960) is formulated. The state vector of relative navigation algorithm in the spherical coordinates is defined as

$$\mathbf{x} = [\rho \ \ \theta \ \ \phi \ \ \dot{\rho} \ \ \dot{\theta} \ \ \dot{\phi}]^T \qquad (2)$$

After the coordinate transformation with an absolute navigation solution of chief, the state vector is propagated
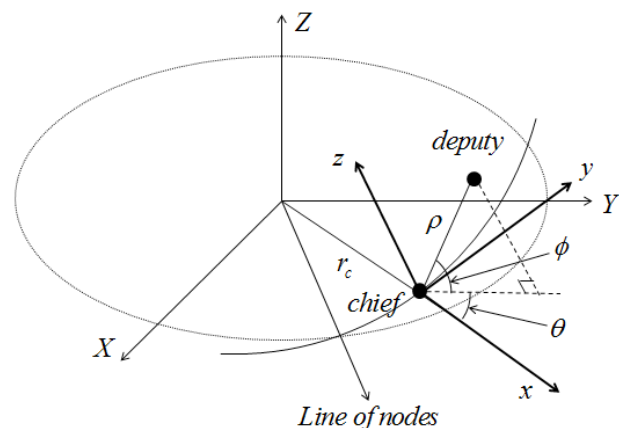

Fig. 1. ECI and relative frames.

in the Earth-Centered Inertial (ECI) frame by following the dynamic model to accommodate the nonlinear and perturbation terms easily:

$$\ddot{\mathbf{r}} = -\frac{\mu_E}{r^3}\mathbf{r} + \mathbf{a}_{J_2} \tag{3}$$

where $\mathbf{r}$ is the position vector of the spacecraft in the ECI frame, μ_E is Earth's gravitational parameter, and $\mathbf{a}_{J_2}$ is the acceleration caused by the J_2 gravitational perturbation. Note that the perturbation terms in the dynamic model are simplified from those stated in Jung et al. (2012), which include the perturbations by the asymmetry of Earth's gravitational potential, air-drag, third bodies (Sun and Moon), and solar radiation pressure. Since the J_2 perturbation dominates in the Low Earth Orbit (LEO) which is considered for the chief and deputy orbit, the perturbation is only used for the proposed algorithm to reduce the computational burden. In the EKF, the covariance matrix P is propagated from the $(k\text{-}1)$-th to the k-th step as follows:

$$\Phi_{k-1} = E + A_{k-1}dt$$
$$P_k^- = \Phi_{k-1}P_{k-1}^-\Phi_{k-1}^T + Q \tag{4}$$

where A is the Jacobian matrix of relative motion, Q is the process noise matrix, and E is the identity matrix. Once the Kalman gain K_k is obtained from Eq. (5), the propagated relative state vector and covariance, $\mathbf{X}_k^-$ and P_k^-, are updated to be $\mathbf{X}_k^+$ and P_k^+:

$$K_k = P_k^- H_k^T (H_k P_k^- H_k^T + R)^{-1} \tag{5}$$
$$\mathbf{x}_k^+ = \mathbf{x}_k^- + K_k[\mathbf{z}_k - \mathbf{h}(\mathbf{x}_k, t_k)]$$
$$P_k^+ = [E - K_k H_k]P_k^- \tag{6}$$

where z is the observation vector, and R is the measurement noise matrix, $\mathbf{h}(\mathbf{x},t)$ is the measurement model, and H is the Jacobian matrix of $\mathbf{h}(\mathbf{x},t)$. When only the laser measurement is used, the observation vector can be defined as $\mathbf{z} = [\rho\,\theta\,\phi]^T$. The azimuth and elevation angle measurements are obtained using the attitude estimation results. Then, the measurement model $\mathbf{h}(\mathbf{x},t)$ using only laser measurements can be expressed as

$$\mathbf{h}(\mathbf{x},t) = \begin{bmatrix} 1 & 0 & 0 & sf & 0 & 0 \\ 0 & 1 & 0 & 0 & 0 & 0 \\ 0 & 0 & 1 & 0 & 0 & 0 \end{bmatrix}\mathbf{x} = H\mathbf{x} \tag{7}$$

where sf is a scale factor to represent the drift due to the range rate (Jung et al. 2012).

2.2 Laser-based Navigation Algorithm with Modified Measurement Model Employing GPS Pseudo-range Measurements

As an effort to overcome the limited accuracy caused by relatively inaccurate attitude estimation, a combined navigation algorithm is proposed by incorporating GPS pseudo-range measurements into the measurement model presented in the previous section (Eq. (7)). The pseudo-range pr and carrier phase measurement cph from single frequency (L1) GPS receivers are modeled as follows (Hofmann-Wellenhof et al. 2012):

$$pr = p + c(\delta t - \delta t_{GPS}) + I$$
$$cph = p + c(\delta t - \delta t_{GPS}) + N\lambda - I$$
$$p = |\mathbf{r} - \mathbf{r}_{GPS}| \tag{8}$$

where I is the delay due to the ionospheric effects, $c = 3\times10^8\,m/s$ is the speed of light, $\mathbf{r}_{GPS}$ is the position vector of the GPS satellite, N is the carrier phase ambiguities, λ is the wavelength of the GPS signal, δt is the clock bias of the GPS receiver, and δt_{GPS} is the clock bias of the GPS satellites. The observation vector is composed of the range measured by a laser and the single difference of pseudo-range measurements between the chief and deputy instead of the azimuth and elevation angles.

$$\mathbf{z} = [\rho\,\,\Delta pr_1\,\,\cdots\,\,\Delta pr_n]^T \tag{9}$$

where n is the number of GPS satellites transmitting signals to both the chief and deputy satellites. The state vector for relative navigation is redefined by including $\Delta\delta t$, which is the difference between the GPS receiver clock bias in the chief and deputy.

$$\mathbf{x} = [\rho\,\,\theta\,\,\phi\,\,\dot{\rho}\,\,\dot{\theta}\,\,\dot{\phi}\,\,\Delta\delta t]^T \tag{10}$$

Then, the modified measurement model can be obtained as

$$\mathbf{h}(\mathbf{x},t) = \begin{bmatrix} \rho + sf\,\dot{\rho} \\ h_{1,GPS}(\mathbf{x},t) \\ \vdots \\ h_{n,GPS}(\mathbf{x},t) \end{bmatrix}$$
$$h_{j,GPS}(\mathbf{x},t) = |\mathbf{r}_c + \Delta\mathbf{r}(\mathbf{x},t) - \mathbf{r}_{j,GPS}| - |\mathbf{r}_c - \mathbf{r}_{j,GPS}| + c\Delta\delta t \tag{11}$$

where $\mathbf{r}_c$ is the position vector of the chief and $\Delta\mathbf{r}$ is the difference of position vectors between the chief and deputy which can be expressed by Eq. . Based on Eq. (12), the Jacobian matrix of the measurement model can be obtained

numerically.

$$H = \begin{bmatrix} \dfrac{\partial}{\partial \mathbf{x}}(\rho + sf\dot{\rho}) \\ \dfrac{\partial h_{1,GPS}}{\partial \mathbf{x}} \\ \vdots \\ \dfrac{\partial h_{n,GPS}}{\partial \mathbf{x}} \end{bmatrix} = \begin{bmatrix} \dfrac{\partial}{\partial \mathbf{x}}(\rho + sf\dot{\rho}) \\ \dfrac{\partial}{\partial \mathbf{x}}\left(\left|\mathbf{r}_c + \Delta\mathbf{r}(\mathbf{x},t) - \mathbf{r}_{1,GPS}\right| + c\Delta\delta t\right) \\ \vdots \\ \dfrac{\partial}{\partial \mathbf{x}}\left(\left|\mathbf{r}_c + \Delta\mathbf{r}(\mathbf{x},t) - \mathbf{r}_{n,GPS}\right| + c\Delta\delta t\right) \end{bmatrix} \quad (12)$$

In order to increase the accuracy of the navigation algorithm, the pseudo-range measurements are smoothed by the Kalman filter using carrier phase measurements (Montenbruck et al. 2002).

$$pr_k^- = pr_{k-1} + [cph_k - cph_{k-1}]$$
$$pr_k^+ = pr_k^- + G[pr_k - pr_k^-] \quad (13)$$

where pr_{k-1} is the previous filter output of pseudo-range measurement, cph_{k-1} is the previous carrier-phase measurement, pr_k^- is the propagated pseudo-range, and G is the Kalman gain for smoothing the propagated pseudo-range. G is obtained by the following relationship with design parameter n_{lim} (Montenbruck et al. 2002):

$$G = \begin{cases} 1/k \\ 1/n_{lim} \end{cases} for \begin{cases} k < n_{lim} \\ k \geq n_{lim} \end{cases} \quad (14)$$

Fig. 2 shows a flowchart of the proposed navigation algorithm. As shown in Eq. (9) and Fig. 2, this proposed algorithm does not require azimuth and elevation angles as the observation vector, thus it is independent of the attitude estimation error. The relative navigation error does not increase even in case of poor attitude estimation.

3. RESULT AND ANALYSIS

The proposed navigation algorithm is applied to the deputy spacecraft with respect to the chief on LEO. The navigation algorithms presented in Montenbruck et al. (2002) and Jung et al. (2012), which use only laser measurements and only GPS measurements, respectively, are also applied to the same problems for comparative analyses. The laser measurements are simulated by the software model based on the femtosecond laser instrument presented in Jung et al. (2012) and Jang et al. (2014), which is expected to yield the range with **μ**m to cm-level accuracy
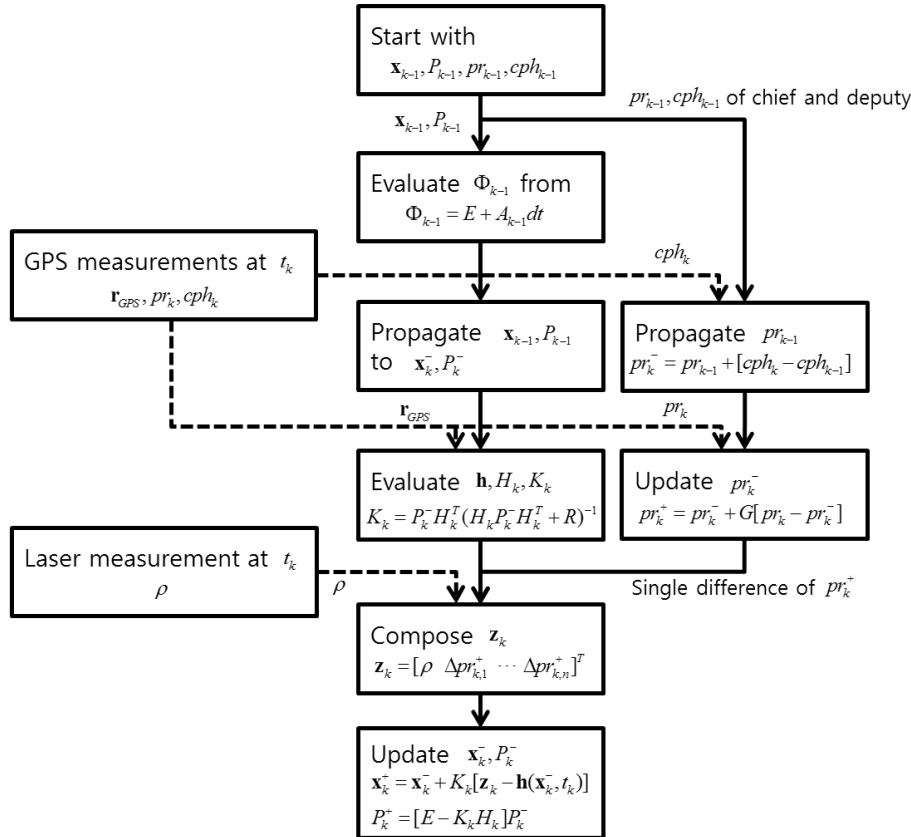

Fig. 2. Flowchart of laser-based relative navigation algorithm using GPS measurements.

depending on the relative distance. We set the phase measurement noise of the laser instrument in the software model as Gaussian noise with $1\sigma = 0.01°$ to consider the uncertainty and specification of the hardware. The actual GPS RF signal is generated by Spirent Communications' GSS 6560 simulator, and is received through the spaceborne GPS L1 single-frequency receiver (AsteRX1 PRO) manufactured by Septentrio Inc. The true orbits of the chief and deputy are generated by numerical integration of the dynamic model defined in the ECI frame. The dynamic model includes those perturbations by the asymmetry of Earth's gravitational potential, air-drag, third bodies (Sun and Moon), and solar radiation pressure.

3.1 Relative Navigation Results in Large-scale Formation Flying

The relative orbit determination examples for demonstration are set as the relative orbits with 50 km and 200 km radii. The initial conditions of the chief and deputy are given in the ECI frame as

$Chief$: $\mathbf{r} = [6930 \quad 0 \quad 0\,]\,km$, $\mathbf{v} = [0 \quad 3.811 \quad 6.601]\,km/s$
$Deputy\,(50\,km)$: $\mathbf{r} = [6955 \quad -43.301 \quad 25\,]\,km$, $\mathbf{v} = [0 \quad 3.797 \quad 6.577]\,km/s$
$Deputy\,(200\,km)$: $\mathbf{r} = [7030 \quad -17.321 \quad 100\,]\,km$, $\mathbf{v} = [0 \quad 3.757 \quad 6.506]\,km/s$ (15)

The initial conditions of the deputy are set to be the solutions of the Hill–Clohessy–Wiltshire (HCW) equations for implementing the projected circular orbits, which are circular when projected onto the radial direction of the relative frame. After separation of the terms in the weighting matrices into the types of states and measurements, the weighting matrices are empirically determined by adjusting the terms one by one to improve the accuracy.

$Q = \text{diag}([10^{-4} \quad 10^{-14} \quad 10^{-14} \quad 10^{-8} \quad 10^{-18} \quad 10^{-18} \quad 10^{14}]^T)$
$R = \text{diag}([10^{-11} \quad 10^{-3} \quad \cdots \quad 10^{-3}]^T)$, $n_{\lim} = 50$ (16)

Figs. 3–4 and 5-6 show the estimation errors of relative states by the proposed navigation algorithm in the case of 50 km and 200 km radius, respectively. They are represented in spherical and rectangular coordinates. The relative states converge well in both spherical and rectangular coordinates. The tendencies of the converged errors are presented in Figs. 3–4 and 5-6, and are similar to each other because of the same dynamical environments, initial conditions of the chief, and modeling of the GPS/laser measurements in the numerical simulations. Tables 1 and 2 present the Root Mean Square (RMS) errors of relative states from each navigation algorithm for the case of 50 km and 200 km radius, respectively. The accuracies of the azimuth

and elevation angles for the algorithm using only laser measurements are set as 1 arcsec, 0.001°, 0.005°, and 0.01° for the simulation examples. The estimation errors of the proposed algorithm are lower than those of the algorithm using only laser measurements even in the case of 0.001° accuracy in both cases. The proposed algorithm also shows more accurate results than the algorithm using only GPS measurements. Note that the state-of-the-art star trackers, the most accurate sensors for attitude estimation, have an accuracy of 2–10 arcsec (Ma et al. 2013). This implies that the proposed algorithm can yield more accurate navigation solutions than the algorithm using only laser measurements in large-scale formation flying, even though the spacecraft is equipped with the star tracker. Moreover, the azimuth and elevation errors must be greater than or equal to the attitude estimation errors due to the numerical and systematic errors accumulated through the coordinate transformations, which clearly demonstrates the advantage of the proposed
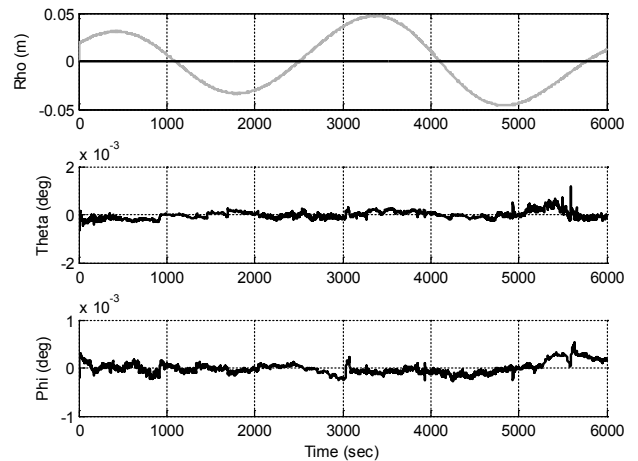
Fig. 3. Estimation errors of relative states (black line) and observation errors of laser measurements (grey line) in spherical coordinates for a radius of 50 km.
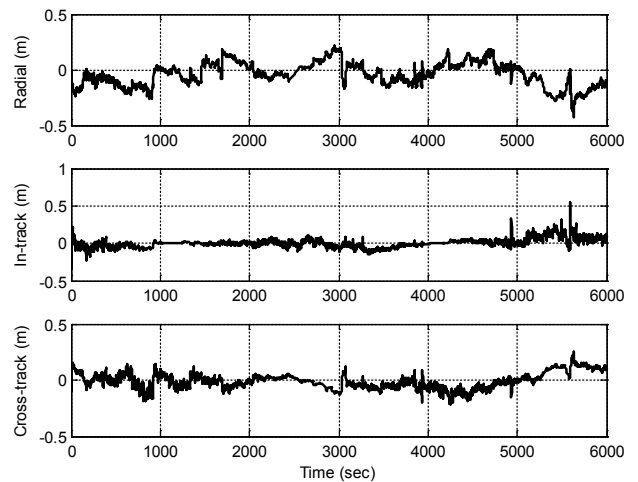
Fig. 4. Estimation errors of relative states in rectangular coordinates for a radius of 50 km.
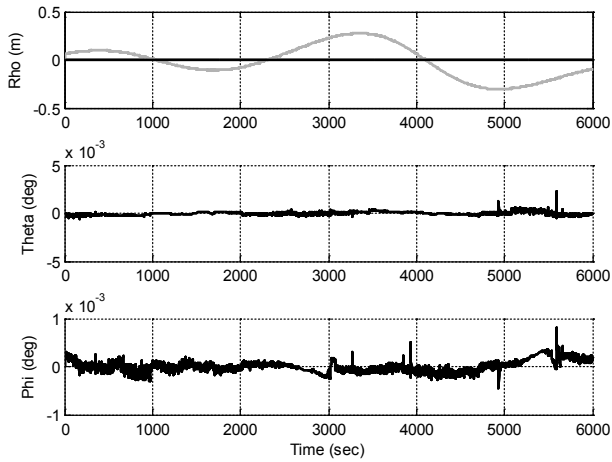
Fig. 5. Estimation errors of relative states (black line) and observation errors of laser measurements (grey line) in spherical coordinates for a radius of 200 km.
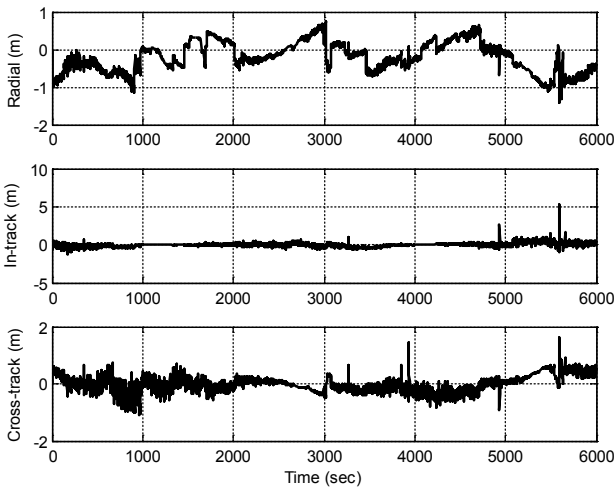

Fig. 6. Estimation errors of relative states in rectangular coordinates for a radius of 200 km.

Table 1. Relative position RMS errors of navigation algorithms for a radius of 50 km

Algorithm	Radial (cm)	In-track (cm)	Cross-track (cm)	3D (cm)	1σ error of angular measurements
Laser+GPS	11.54	5.678	7.308	14.80	-
Laser only	5.374	3.363	4.439	7.739	1 arcsec
Laser only	12.00	6.646	9.856	16.89	0.001 deg
Laser only	32.15	22.50	32.80	51.15	0.005 deg
Laser only	59.84	36.68	53.10	88.01	0.01 deg
GPS only	14.43	10.01	8.608	19.56	-

Table 2. Relative position RMS errors of navigation algorithms for a radius of 200 km

Algorithm	Radial (cm)	In-track (cm)	Cross-track (cm)	3D (cm)	1 error of angular measurements
Laser+GPS	44.02	25.06	28.71	58.23	-
Laser only	20.49	13.71	16.45	29.64	1 arcsec
Laser only	49.73	32.60	41.02	72.25	0.001 deg
Laser only	149.2	123.7	150.9	245.7	0.005 deg
Laser only	519.9	503.7	266.0	771.2	0.01 deg
GPS only	56.17	37.80	32.80	75.23	-

algorithm independent of the attitude estimation error in practical cases.

3.2 Analyses for Navigation Strategy

The superiority of the proposed algorithm to the algorithm using only laser measurements depends on both relative distance and attitude accuracy. Based on the 3-dimensional relative position RMS errors with respect to the relative distances and attitude accuracies, the formulae which provide the timing for switching between the proposed algorithm and the algorithm using only laser measurements can be empirically deducted.

The 3-dimensional relative position RMS errors are obtained by numerical simulations in the case of 1 km, 10 km, 30 km, 50 km, 100 km, and 200 km relative distances. The attitude accuracies are set to be the same as those in Section 3.1. These results lead to estimation of the critical accuracy of angular measurement at which the position RMS error of the proposed algorithm is the same as that of the algorithm using only laser measurements for each distance. The upper panel in Fig. 7 shows the critical accuracy vs. relative distance, which converges to a value less than 0.001°. When these critical accuracies are multiplied by each relative distance, the resultant values are almost proportional to the relative distances. The lower panel in Fig. 7 shows these values and their linear approximations (dashed line). This tendency allows us to define the decision parameter d_c which is the multiplication of the accuracy of primary attitude sensor and the relative distances. Using this d_c, the timing can be estimated for switching between the proposed algorithm and the algorithm using only laser measurements as follows:
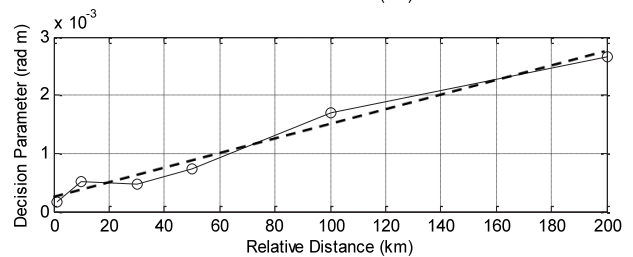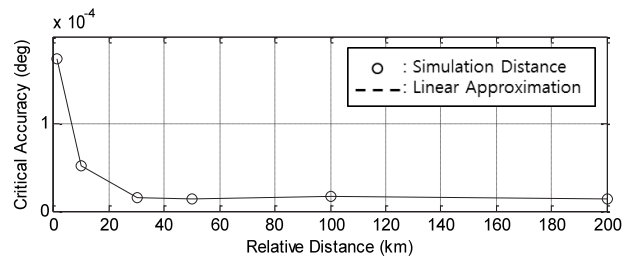

Fig. 7. Critical accuracy and its relationship to relative distances.

$$\begin{cases} Laser \\ Laser \ and \ GPS \end{cases} for \begin{cases} d_c < 0.012\left|\Delta\mathbf{r}\right| + 0.23 \\ d_c \geq 0.012\left|\Delta\mathbf{r}\right| + 0.23 \end{cases} \quad (17)$$

4. CONCLUSION

In this paper, a combined navigation algorithm using laser and GPS measurements for large-scale formation flying is proposed. Based on the algorithm presented by Jung et al. (2012), the relative navigation algorithm is formulated by modifying the measurement model. The single difference of GPS pseudo-range measurements is incorporated into the measurement model instead of the azimuth and elevation angles. The extended Kalman filter is applied to estimate the relative position and velocity and to obtain the smoothed pseudo-range measurements to increase the accuracy of the algorithm. This strategy allows the laser-based relative navigation algorithm to exclude angular measurements of laser directions which depend on attitude estimation errors, so the proposed algorithm can provide better relative navigation results than the algorithm using only laser measurements with attitude accuracies greater than 0.001° in large-scale formation flying. Considering the accuracy of the state-of-the-art star trackers and the accumulated errors in the transformation between azimuth/elevation and attitude information, it is clearly demonstrated that the proposed algorithm can be considered favorably compared with the algorithm using only laser measurement in large-scale formation flying.

ACKNOWLEDGMENTS

REFERENCES

Ardaens JS, D'Amico S, Montenbruck O, Flight Results from the PRISMA GPS-Based Navigation, in 5th ESA Workshop on Satellite Navigation Technologies, Noordwijk, Netherlands, 8-10 Dec 2010.

Hofmann-Wellenhof B, Lichtenegger H, Collins J, Global Positioning System: Theory and Practice (Springer, Berlin, 2012).

Jang YS, Lee K, Han S, Lee J, Kim YJ, et al., Absolute distance measurement with extension of nonambiguity range using the frequency comb of a femtosecond laser, Opt. Eng. 53, 122403 (2014). http://dx.doi.org/10.1117/1.OE.53.12.122403

Jung S, Park YS, Park HE, Park C, Kim SW, et al., Real-Time Determination of Relative Position Between Satellites Using Laser Ranging, J. Astron. Space Sci. 29, 351-362 (2012). http://dx.doi.org/10.5140/JASS.2012.29.4.351

Kalman RE, A new Approach to Linear Filtering and Prediction Problems, J. Basic Eng. 82, 35-45 (1960). http://dx.doi.org/10.1115/1.3662552

Kroes R, Montenbruck O, Bertiger W, Visser P, Precise GRACE baseline determination using GPS, GPS Solut. 9, 21-31 (2005). http://dx.doi.org/10.1007/s10291-004-0123-5

Leung S, Montenbruck O, Real-Time Navigation of Formation–Flying Spacecraft Using Global-Positioning-System Measurements, J. Guid. Control Dyn. 28, 226-235 (2005). http://dx.doi.org/10.2514/1.7474

Ma L, Hu C, Wang X, Dai D, Advances and Accuracy Performance of the Star Trackers, Proc. of SPIE 8908 (2013). http://dx.doi.org/10.1117/12.2032690

Montenbruck O, Ebinuma T, Lightsey EG, Leung S, A real-time kinematic GPS sensor for spacecraft relative navigation, Aerosp. Sci. Technol. 6, 435-449 (2002). http://dx.doi.org/10.1016/S1270-9638(02)01185-9

Park HE, Park SY, Kim SW, Park C, Integrated orbit and attitude hardware-in-the-loop simulations for autonomous satellite formation flying, Adv. Space Res. 52, 2052-2066 (2013). http://dx.doi.org/10.1016/j.asr.2013.09.015

Park JI, Park HE, Park SY, Choi KH, Hardware-in-the-loop simulations of GPS-based navigation and control for satellite formation flying, Adv. Space Res. 46, 1451-1465 (2010). http://dx.doi.org/10.1016/j.asr.2010.08.012

Shaddock DA, Space-based gravitational wave detection with LISA, Class. Quantum Grav. 25, 114012 (2008). http://dx.doi.org/10.1088/0264-9381/25/11/114012

Sheard BS, Heinzel G, Danzmann K, Shaddok DA, Klipstein WM et al., Intersatellite laser ranging instrument for the GRACE follow-on mission, J. Geod. 86, 1083-1095 (2012). http://dx.doi.org/10.1007/s00190-012-0566-3

Wang X, Gong D, Xu L, Shao X, Duan D, Laser radar based relative navigation using improved adaptive Huber filter, Acta Astronaut. 68, 1872-1880 (2011). http://dx.doi.org/10.1016/j.actaastro.2011.01.002